ISSN 1024-8560, Atmospheric and Oceanic Optics, 2023, Vol. 36, No. 2, pp. 176–184. © The Author(s), 2023. This article is an open access publication.
Russian Text © The Author(s), 2022, published in Optika Atmosfery i Okeana.

ATMOSPHERIC RADIATION, OPTICAL WEATHER, AND CLIMATE

Black Carbon Seasonal Trends and Regional Sources on Bely Island (Arctic)

O. B. Popovicheva[a, *], M. A. Chichaeva[b, **], V. O. Kobelev[c, *], and N. S. Kasimov[b, ****]**

[a] *Skobeltsyn Institute of Nuclear Physics, Moscow State University, Moscow, 119991 Russia*
[b] *Faculty of Geography, Moscow State University, Moscow, 119991 Russia*
[c] *Russian Geographic Society, Moscow Branch, Moscow, 109012 Russia*
**e-mail: olga.popovicheva@gmail.com*
***e-mail: machichaeva@gmail.com*
****e-mail: vasily.kobelev@gmail.com*
*****e-mail: nskasimov@mail.ru*

Received August 3, 2022; revised August 25, 2022; accepted October 25, 2022

Abstract—The impact of aerosol sources on the pollution of the Russian sector of the Arctic is now strongly underestimated. A new polar aerosol station was arranged in August 2019 on Bely Island (Kara Sea), on the pathway of air mass transport from industrial regions of Western Siberia to the Arctic. Continuous aethalometer measurements of a short-lived climate tracer, i.e., black carbon, (from December to April 2019 and from January to November 2020) showed its seasonal variations with high values (60–92 ng/m^3) in December–April and low values (18–72 ng/m^3) in June–September. Pollution periods are identified. Regional distribution of fossil fuel and biomass combustion sources are obtained using the black carbon concentration weight trajectory model. The impact of gas flaring from oil and gas extraction areas of Western Siberia, the Volga region, the Urals, and the Komi Republic is found to be most pronounced during the cold period, and the impact from wildfire smoke emissions is found to be maximal in the warm season. A marker of biomass burning impact, determined from the difference between the black carbon concentrations measured in a broad wavelength spectrum, indicated the predominant effects from residential wood combustion in the cold period and agricultural and forest fires in the warm season.

Keywords: the Arctic, black carbon, emission, fossil fuel combustion, wildfire, seasonal trend
DOI: 10.1134/S1024856023030090

INTRODUCTION

Climate changes due to aerosol pollution of the atmosphere present a serious problem worldwide. Industrialization and population growth act to increase the amount of aerosol substances emitted to the atmosphere and the frequency of large-scale wildfires. The Arctic region is most vulnerable to fossil fuel and biomass combustion emissions. The Arctic haze phenomenon [1] is observed in the winter–spring period as a result of a combination of intense long-range transport of anthropogenic emissions from low latitudes and temperature inversion. As the sunlight increases in intensity in spring, the atmosphere becomes less stable, the aerosol concentration decreases, and the effect from local sources in coastal regions of the Arctic intensifies as compared to the winter.

Black carbon (BC) in the composition of combustion products absorbs solar radiation well; BC is a short-lived climatically significant constituent which appreciably influences the climate of the Arctic [2]. The combined effect of BC and atmosphere-cooling sulfates increases the Arctic surface temperature by +0.29 K and makes ~20% of all factors of the Arctic warming since the early 1980s [3]. The BC accumulation in the lower troposphere intensifies the energy exchange between clouds and snow cover [4]. The BC deposition on snow acts to decrease the surface albedo and speed up snow and ice melt [5].

A high-molecular-weight organic carbon, also called brown carbon (BrC), absorbs UV solar radiation, exhibiting strong differences between smokes from wood combustion and motor vehicle exhausts [6, 7]. Accumulating in the Arctic aerosols after transport of fire-emitted smokes, BrC appreciably contributes to the warming of the atmosphere over the region with radiative forcing of ~30% relative to BC [8].

The atmosphere of the high-latitude Arctic (poleward of 66° N) receives up to 62% of BC from Russian territories [9]. Aircraft measurements confirm that the tropospheric BC over the coast of Russian Arctic seas strongly varies in space and time, with its anthropogenic sources being predominant [10]. Despite the

reduction in anthropogenic emissions over recent decades [11], observations of seasonal BC cycles at 10 polar observatories, including the Tiksi International Hydrometeorological Observatory (HMO, coast of the Laptev Sea, Eastern Siberian sector of the Arctic), demonstrated the yearly recurring wintertime phenomenon, i.e., Arctic haze. Plumes from wildfires are recorded in the spring–summer seasons in coastal forested regions of the Arctic [12]. The BC transport by plumes from fires during summer was recorded in measurements of physicochemical characteristics of aerosol at Polar Station Ice Base Cape Baranov (Severnaya Zemlya Archipelago, Eastern Siberian sector of the Arctic) [13, 14]. Agricultural fires in the European part of the Russian Federation and in the south of Siberia are a significant source of emissions and pollutants in the Arctic [15].

Due to large amounts of pollutants emitted and proximity to the region under study, gas flaring during oil and gas extraction [16] accounts for as much as 42% of the annual mean BC concentrations in the Arctic [17]. The largest oil and gas production areas in Western Siberia and the northeast of the European Russia, located on the air mass transport pathway to the Arctic, introduce a disproportionately large contribution to the pollution of the Arctic troposphere [18, 19]. As a result of pollutant plume outflows from these regions to the seas of the Arctic Ocean, the BC concentrations increase to 400 ng/m^3 as compared to the level of few ng/m^3 under the opposite wind direction [20]. However, estimates of the contributions from gas flaring emissions at the polar stations operating in the European and Canadian sectors of the Arctic are unreliable because they are far removed from industrial sources [17], and because the existing models reproduce the BC concentrations in the Arctic region with a large uncertainty [21].

The high BC concentrations, measured at the Tiksi HMO, are caused by the residential emissions and long-range transport from industrial regions predominantly in winter–spring period; lower concentrations during summer result from biomass burning during wildfires [22]. Radiocarbon analysis data from Tiksi HMO show that fossil fuel combustion contributes 32 ± 16% more than biomass burning [23]. Previously, it was shown [24] that the transport dispersion model of particles coupled with the inventory of anthropogenic emissions and biomass burning emissions accurately determines the contributions of BC sources in the European sector of the Arctic. However, this model gave a surprisingly small contribution of ~6% from gas flaring emissions for the Tiksi HMO, mostly due to uncertain data on the spatial distribution of BC sources over the territory of Siberia, the absence of an emission inventory, and the large distance of the station from gas and oil production regions.

Complex measurements of the properties of Arctic aerosols, including aerosol absorptance in a wide solar radiation spectrum, are required to estimate the climatic consequences of emissions of carbon-containing aerosols. A new polar aerosol research station on Bely Island in the Kara Sea (Yamalo-Nenets Autonomous Okrug (YNAO), Western Siberian sector of the Arctic, https://peexhq.home.blog/2019/12/11/new-research-aerosol-stations-in-the-russian-arctic), owned by Moscow State University (MSU), was installed in 2019 to carry out long-term complex observations of the composition of the Arctic atmosphere and to estimate the influence of emissions from the oil and gas extraction sector. Three-month continuous measurements of the BC mass concentrations were preliminarily conducted at an aerosol complex near Salekhard [25]. The station is located in the north of the YNAO on the pathway of the outflow of large-scale emissions from industrial regions of Western Siberia and densely populated and industrial regions of Eurasia to the Arctic and, as such, provides a unique opportunity for studying the aerosol pollution of the atmosphere of the Western Siberian sector of the Arctic [26].

The purpose of this work is to analyze the measurements of the BC concentration carried out with the instrumental complex at Bely Island station and to study the distribution of pollution sources of Arctic aerosols on Bely Island in the cold and warm time of the year.

MEASUREMENTS AND DATA PROCESSING

Bely Island is in the Kara Sea and separated from the Yamal Peninsula by Malygina Strait. The annual average temperature is −10.6°C. Winters are long and cold: the average temperature is −24.2°C (occasionally reaching −59°C) in February, fogs are typical during summer, and the average air temperature is +5.3°C. The monthly precipitation amount is more than 20 mm.

We analyze the observations from August to December 2019 and from January to November 2020. The period from November 1, 2019, to April 1, 2020, as well as November 2020, when the temperature dropped below −10°C, is conventionally designated as cold and the remainder as warm. The cold period was dominated by continental (S–SE) winds. From June to September, the average temperature was kept above 0°C and N–NE winds were predominant, which determined the predominance of oceanic air masses that came from the Arctic Ocean area. The air temperature decreased and stayed below 0°C in October due to lower insolation. The average wind speed over the observation period was 5–10 m/s.

The MSU research station Bely Island has been continuously operated since August 2019. Its position in the north of Western Siberia (73°20′7.57″ N, 70°4′49.05″ E) relative to the Arctic stations Zeppelin, Alert, Barrow, Summit, Tiksi, and Ice Base Cape Baranov is shown in Fig. 1. The pavilion of the aerosol

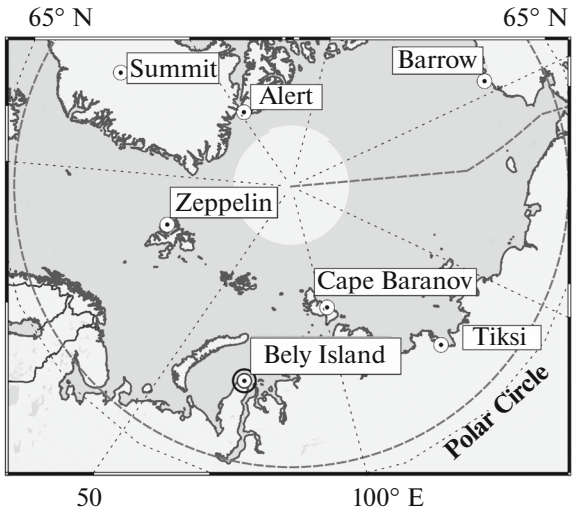

Fig. 1. Map of polar aerosol stations.

complex is approximately half a kilometer to the southeast of the hydrometeorological station, where a diesel generator operates, the only local pollution source on the island. The measurements made when wind blew from the direction of the station were sorted out of the dataset. The isolation of the Bely Island station from anthropogenic sources is the main advantage of instrumental complex over the Tiksi HMO, which is significantly affected by emissions from the nearby Tiksi settlement [22].

In the station pavilion, a continuous sampling system is mounted, which has been designed for use under severe Arctic conditions. An aethalometer AE33 (Magee Scientific, Aerosol d.o.o.) is used to determine the absorptance of particles that deposit on filter after air is pumped through with different flow speeds, which give the coefficient of correction for absorption inside the filter [27]. The measurements are carried out at seven wavelengths in the range from ultraviolet (370 nm) to infrared (950 nm) with a resolution of 1 min. The absorption efficiency at a wavelength of 880 nm is recalculated into the equivalent black carbon concentration eBC (880) with a mass coefficient of 7.7 m^2/g. The spectral dependence of absorption makes it possible to take into account the absorption by high-molecular organic carbon in the ultraviolet region increased as compared to the infrared [28]. The difference between eBC (370) and eBC (880), called the Delta-C parameter, turns out to be considerable in biomass burning emissions [29, 30]. In this work, the parameter Delta-C is used as an indicator of the effect of residential wood combustion and wildfires.

Background aerosol concentrations in the Arctic region are determined in the absence of the effects of local and regional pollutions [22, 31]. The value of 10 ng/m^3, equaling 20 percentiles of the sample throughout the measurement period, was taken as the background concentration in this work. Long-term events, during which the concentrations eBC exceeded a threshold of 90 nm/m^3, equal to the 80th percentile of the sample, are identified as pollution episodes.

To determine the impact zone of the possible sources of BC emissions on pollution level on Bely Island, the HYSPLIT model, Air Resources Laboratory [32], was used to calculate the array of back trajectories of air mass transport throughout the observation period with a time interval of 1 h and 240 h backward at altitudes of 100 and 500 m above the ground level (AGL) with a spatial resolution of 1° latitude and 1° longitude. Based on this, we carried out the cluster analysis of similar in origin and close trajectories, with the angular distances used as a criterion for clustering [33]. A trajectory calculated by averaging angular distances over all trajectories represents a given cluster.

The method of referencing the air mass transport trajectories to the pollutant concentration at time of their arrival at the observation site, i.e., Concentration Weight Trajectories (CWT) method, is an efficient tool for analyzing atmospheric pollutant transport and identifying their possible pollution sources [34]. Spatial sources are determined by calculating the pollutant concentrations C_{ij} for each grid cell (i, j):

$$\ln(\bar{C}_{ij}) = \frac{1}{\sum_{k=1}^{N} \tau_{ijk}} \sum_{k=1}^{N} \ln(C_k)\tau_{ijk}, \quad (1)$$

where i and j are the latitude and longitude of the cell; k is the index of the trajectory; N is the total number of the calculated trajectories; C_k is the concentration measured at time when kth trajectory arrives at the measurement site; and τ_{ijk} is the time while the kth trajectory is within the cell (i, j).

The fields of the concentrations C_{ij} received from long-term observations make it possible to interrelate high C_k values and the trajectories of air mass motion, thus showing spatial regions with increased emission intensity and probable location of the source. In this work, the regional distribution of BC sources was determined by referencing the trajectories calculated throughout the observation period to the concentration at time of arrival at the Bely Island station. The method is based on joint analysis of air mass transport trajectories and aethalometer measurements of the concentrations eBC.

Locations of gas flares were determined using MODIS and VIIRS satellite data on the glow of structures with temperature higher than 1200°C, corresponding to the gas flaring combustion (https://viirs.skytruth.org/apps/heatmap/). Data on fire activities were received from the Fire Information for Resource Management System (FIRMS) created by the NASA/GSFC Earth Science Data Information Sys-

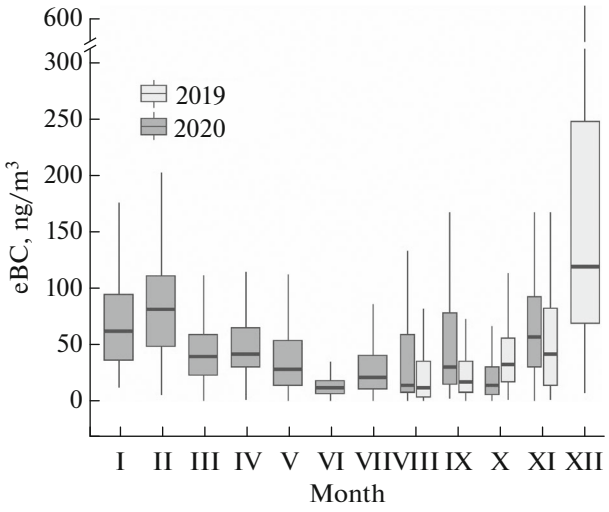

Fig. 2. Monthly dynamics of median concentrations eBC in 2019 and 2020. Height of boxes indicates values between the first and third quartiles; vertical (horizontal) lines indicate maximal and minimal (median) values.

tem (https://firms.modaps.eosdis.nasa.gov/map), and satellite sensing of thermally active points on the Earth's surface.

RESULTS AND DISCUSSION

Long-term studies of variations in aerosol constituents at polar stations indicate that there are seasonal trends characteristic for the Arctic [35]. The time series of monthly average eBC values at the Bely Island station is presented in Fig. 2. The concentrations were maximal (as large as 160 ng/m^3) from November to April and minimal (about 20 ng/m^3) from June to August. The Arctic haze was recorded from November 2019 to March 2020. The median concentration was maximal (127 ng/m^3) in December 2019. The concentrations were on the average 10 times lower in summer than in winter, the minimal value of 30 ng/m^3 being observed in July 2020. The second year of observations showed similar features, with concentration level again being low in summer and high in winter. The eBC value reached an anomalously high value of 72 ng/m^3 in September 2020, two times higher than in September 2019.

The monthly eBC showed similar variations in 2015–2016 at Tiksi HMO, with high values (~130–230 ng/m^3) in the winter–spring period and low values (~20 ng/m^3) from May to October [22]. At Ice Base Cape Baranov station in the same period of time during winter, the concentrations were recorded to be 142 ± 120 ng/m^3, with a maximum of 350 ng/m^3 on January 13, 2016, and 67 ± 43 ng/m^3 in summer [13].

Thus, the eBC values at three Russian stations, i.e., Bely Island, Tiksi HMO, and Ice Base Cape Baranov, during Arctic haze were found to be higher than at Alert site, Canada (100 ± 65 ng/m^3), measured in that period, which, in turn, was the highest recorded at all other Arctic stations [36]. This result confirms the conclusions in [37] and [23] that the Siberian Arctic is more contaminated by large-scale emissions from the Eurasian continent than other Arctic regions.

Analysis of daily data in cold and warm periods showed strong eBC variations against background of seasonal behavior (Fig. 3). We single out pollution episodes when eBC exceeds a threshold of 90 ng/m^3. There were eight pollution episodes in the cold period

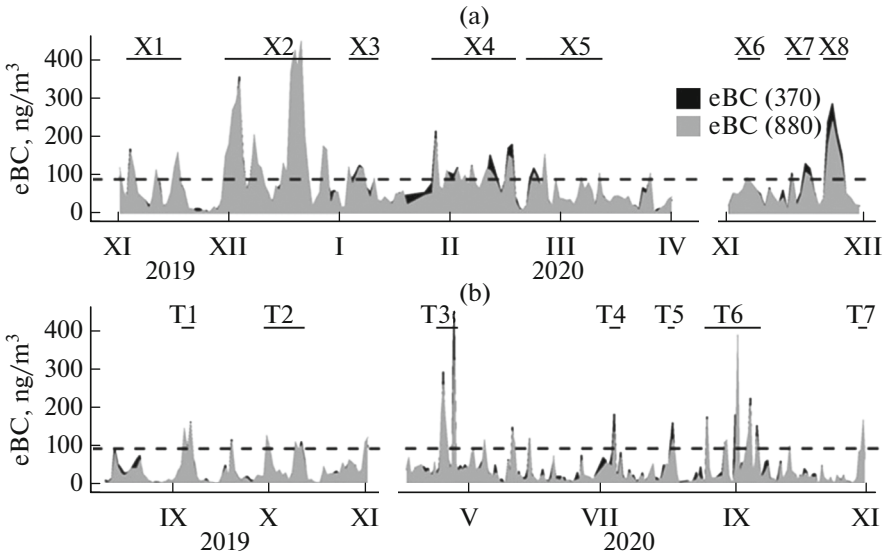

Fig. 3. Daily median eBC (880) and eBC (370) values in (a) cold and (b) warm periods of the year; X1–X8 and T1–T7 are pollution episodes; dashed line indicates an threshold atmospheric pollution value of 90 ng/m^3.

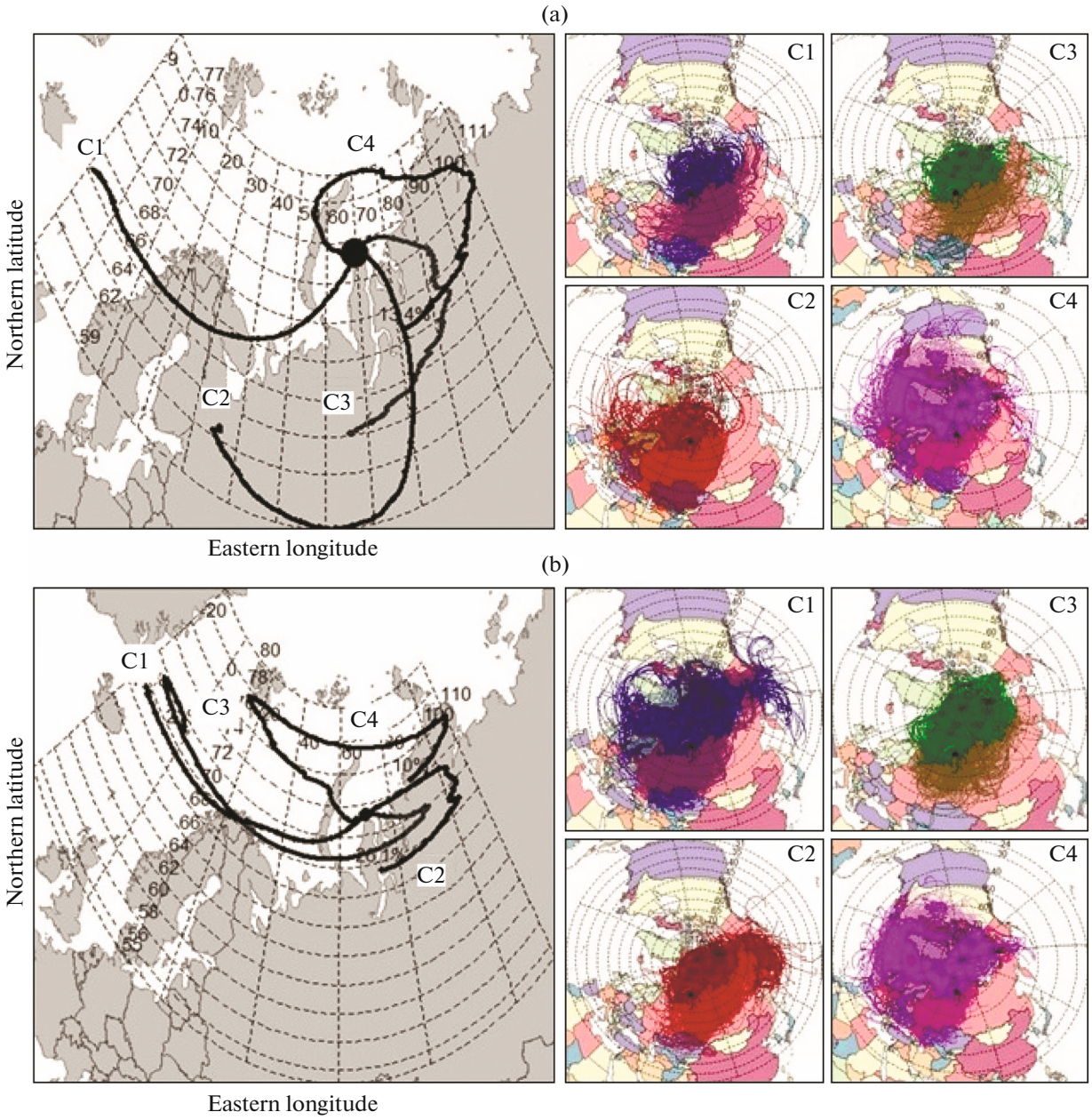

Fig. 4. Calculated average trajectories in clusters C1–C4 (left) and back trajectories of air masses (right) in (a) cold and (b) warm periods of the year; black circle indicates the Bely Island.

(Fig. 3b). High concentrations of eBC occurred thrice during the first episode X1. December 2019 (X2) was characterized by daily maximal eBC values throughout observation period: 350 and 420 ng/m^3 on December 4 and 19. A pollution episode ranked second in intensity (~300 ng/m^3) occurred on November 24 and 25, 2020.

Cluster analysis of back trajectories in the cold period revealed that the impact zone of possible BC sources was mainly in the continental part of Eurasia and had characteristic sizes of few thousand kilometers (Fig. 4). Dominant is C1 cluster of trajectories, which pass through the north of the Scandinavia (Fig. 4a); it comprising 46% of all trajectories over this period. Clusters C2 and C3 encompass vast territories of Eastern Europe, the European part of the Russian Federation, the Urals, Western Siberia, and, partly, Kazakhstan (24 and 16%). Fewer airflows come from subpolar regions of the Arctic Ocean. Air mass transport from Eastern Siberia and from the Arctic Ocean area (cluster C4) turned out to be least significant (13%).

Air mass circulation strongly differs in the warm period. Airflows substantially shift toward the Arctic Ocean coast and encompass the Arctic Ocean area, as

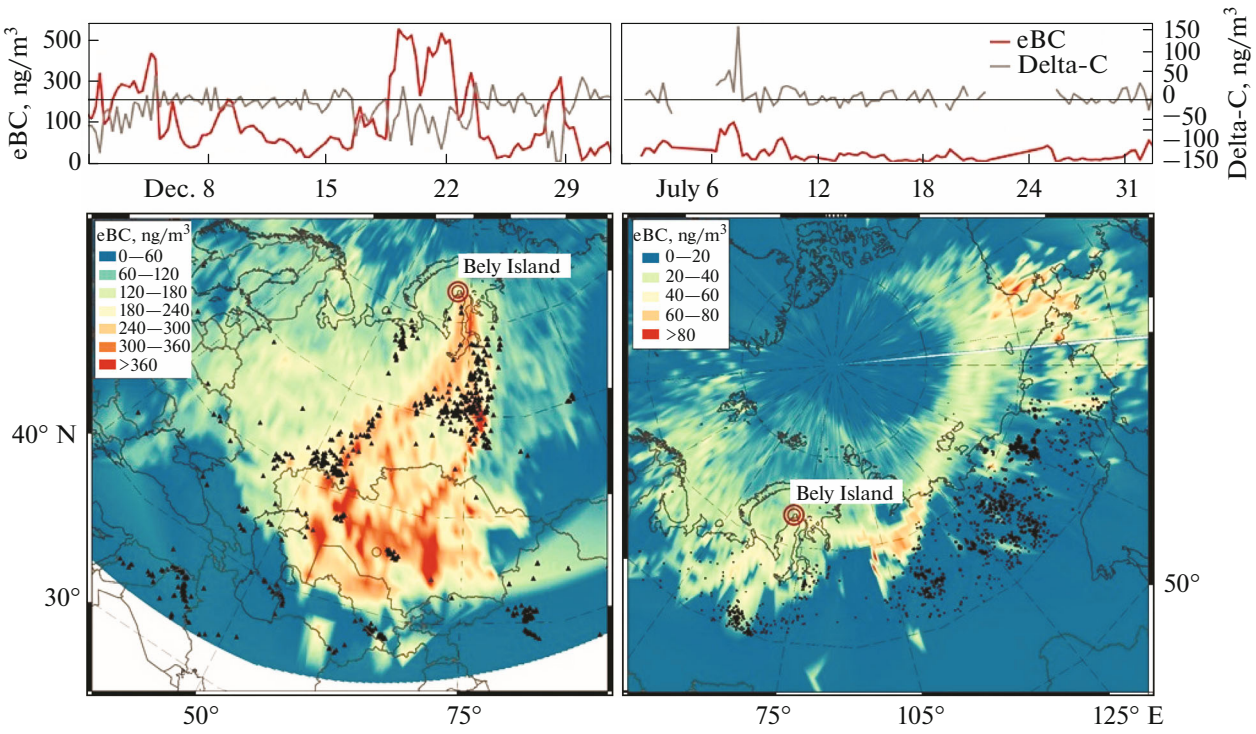

Fig. 5. Concentration eBC and Delta-C on the Bely Island (top) and spatial distribution of BC sources in (a) December 2019 and (b) July 2020; triangles and circles indicate flaring installations in the oil and gas fields and fire centers northward of 60° N, respectively.

well as polar regions of the northern provinces of Canada and Alaska and the regions of the Chukchi Sea and Bering Strait (Fig. 4b). Transport was mostly westerly from the ocean area in the cluster C1 and from the northern territories of the Russian Federation (26 and 23%) in C2 and C3. To a lesser degree, the impact zone was over the continental part of the Eurasian region and island-type Severnaya Zemlya, Spitsbergen, Novaya Zemlya, Franz Josef Land Archipelagos, and Greenland Island; 10% of trajectories from C4 cluster came from the east across the vast region of the Arctic Ocean.

In cold period, eBC (370) was higher than eBC (880) during pollution episodes X4, 5, 7, and 8 (Fig. 5a). They were characterized by the Delta-C values from 20 (November 19, 2020) to 56 ng/m^3 (November 24, 2020) and determined by the prevalence of emissions from wood combustion for the purposes of residential heating in this period of time. We note that, based on the Russian emission inventory, wood combustion accounts for ~61% of the total amount of residential emissions, especially in regions of limited gas utilization [38]. In the warm period, there were low eBC values, rarely exceeding the threshold for pollution episodes (Fig. 5b).

The BC concentration fields, calculated by Eq. (1) using observations at Bely Island station, made it possible to estimate the spatial distribution of the main sources of fossil fuel and biomass combustion emissions in the Eurasian continental part for different seasons. In the cold period of the year, air masses came to Bely Island from densely populated and industrial regions of Eastern Europe, the European part of the Russian Federation, and the Kola Peninsula. The distribution of the eBC sources in December 2019, i.e., in period when the strongest pollutions were recorded, is shown in Fig. 5a. The strongest BC emissions were detected in the Western Siberian and Volga-Ural oil-and-gas bearing basins, i.e., in Khanty-Mansiysk and Yamalo-Nenets Autonomous Okrugs, leading in oil and gas production. Satellite data on locations of gas flares in the largest gas fields indicate that flaring gas combustion is the main source of BC emissions in these regions (Fig. 5a). The regional distribution of BC sources identified in July strongly differs from December distribution in that BC sources are localized predominantly on the coast of the Arctic Ocean (Fig. 5b). In work [39], it was shown that the specific conditions of the atmospheric circulation accompanying Siberian wildfires, may favor reduction of efficiency of transport of atmospheric admixtures to Arctic regions in this period of time.

Biomass combustion has a specific effect on the pollution of the Arctic during the warm period of the year. During our measurements, severe wildfires occurred in the north of Krasnoyarsk Krai, the Republic of Sakha, central and southern Siberia; about 7000000 ha of forest had burned from April to Novem-

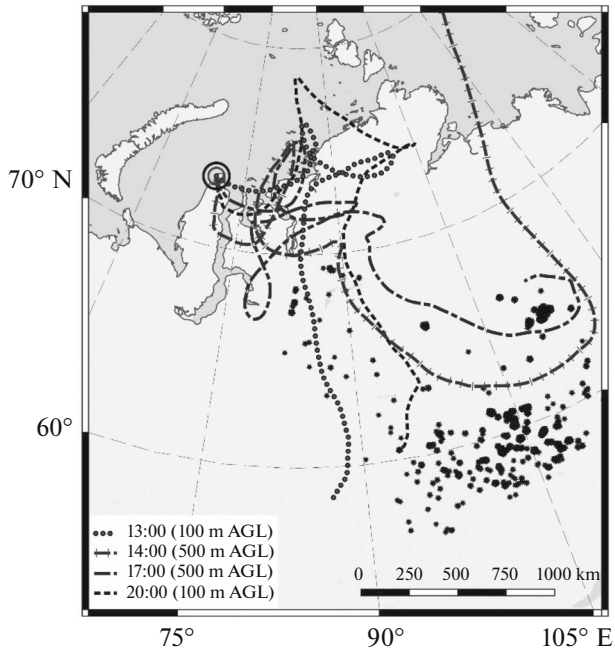

Fig. 6. Back trajectories of air masses on September 1, 2020, at altitudes of 100 and 500 m AGL in the period of pollution episode T6; fires in Krasnoyarsk Krai in the region of trajectory passage.

ber 2020 (https://aviales.ru/popup.aspx?news=6286). Vast agricultural fires in the south of Siberia caused strong springtime pollution T3 (April 18 and 23, 2020), when Delta_C reached 214 ng/m^3 (Fig. 5b), indicating strong contribution of biomass burning. Effect of wildfires was noted in T4 (July 7, 2020), with Delta_C = 100 ng/m^3 (Fig. 5b).

The eBC values were the largest in September 2020 during episode T6 (see Fig. 3b). The maximum eBC (880) = 534 ng/m^3 (September 1, 2020) was a factor of five larger than the threshold value and a factor of 20 larger than the Arctic background level. High values of Delta_C = 209 ng/m^3 indicate the predominant pollution by fire smoke emissions. The trajectory analysis at altitudes of 100 and 500 m AGL for September 1, 2020, points to Krasnoyarsk Krai as a region of sources of numerous fires (Fig. 6).

Thus, outflow of smoke plumes from Siberia regions, namely, Krasnoyarsk Krai and Yakutia, where about one million hectares of forest had burned, entailed unprecedented pollution of the atmosphere of the Arctic in September 2020 by forest biomass burning emissions.

CONCLUSIONS

Continuous measurements of aerosol absorptance in a wide spectral range of solar radiation, carried out at the polar station Bely Island, made it possible to determine for the first time the level of aerosol pollution in the Western Siberian sector of the Russian Arctic from black carbon concentrations. The annual eBC behavior thus obtained is characterized by high values in winter during Arctic haze and low values in summer. For 16 months of observations at Bely Island station we recorded 15 pollution episodes with concentrations reaching 420 ng/m^3 in winter and 534 ng/m^3 in summer. Episodes in the cold period turned out to be longer-lasting, more frequent, and more intense than in the warm period.

The Arctic pollution in the winter–spring period is mainly attributed to long-range air mass transport from low latitudes. A unique position of the aerosol complex on the outflow pathway of large-scale emissions from industrially developed regions made it possible to determine the spatial distribution of gas-flaring emissions as the main source of black carbon on the territories of gas and oil fields in Western Siberia and the Volga-Ural oil-and-gas bearing province, confirmed by satellite data on the locations of gas flares in these regions. The indicator of biomass burning impact showed the predominant influence from residential wood combustion in densely populated regions of Eastern Europe and the European part of the Russian Federation in the cold period and from agricultural and wildfires on the territory of Krasnoyarsk Krai, the Republic of Sakha, and central and southern Siberia in the warm period of the year.

Our data on BC absorptance in a broad spectrum of solar radiation are used to estimate the influence of fossil fuel and biomass combustion sources.

FUNDING

This study was supported by the Russian Science Foundation (project no. 22-17-00-102) and by the Program for Developing Interdisciplinary Research School at Moscow State University "The future of the planet and global environmental changes." The methodology of development of the infrastructure of the aerosol complex is supported by the Ministry of Science and Higher Education of the Russian Federation (project no. 075-15-2021-938).

CONFLICT OF INTEREST

The authors declare that they have no conflicts of interest.

REFERENCES

1. P. K. Quinn, A. Stohl, A. Arneth, T. Bernsten, J. Burhart, J. Christensen, M. Flanner, K. Kupiainen, H. Lihavainen, M. Sheppherd, V. P. Shevchenko, H. Skov, and V. Vestreng, *The Impact of Black Carbon on Arctic Climate (2011)* (Arctic Monitoring and Assessment Programme (AMAP), Oslo, 2011).
2. Q. Wang, D. J. Jacob, J. A. Fisher, J. Mao, E. M. Leibensperger, C. C. Carouge, P. Le Sager, Y. Kondo, J. L. Jimenez, M. J. Cubison, and S. J. Doherty, "Sources of carbonaceous aerosols and deposited black carbon in the Arctic in winter-spring: Implications for radiative forcing," Atmos. Chem. Phys. **11**, 12453–12473 (2011).
3. L. Ren, Y. Yan, H. Wang, R. Zhang, P. Wang, and H. Liao, "Source attribution of Arctic black carbon and sulfate aerosols and associated Arctic surface warming during 1980–2018," Atmos. Chem. Phys. **20**, 9067–9085 (2020).
4. M. G. Flanner, "Arctic climate sensitivity to local black carbon," J. Geophys. Res.: Atmos. **118**, 1840–1851 (2013).
5. P. K. Quinn, T. S. Bates, E. Baum, N. Doubleday, A. M. Fiore, M. Flanner, A. Fridlind, T. J. Garrett, D. Koch, S. Menon, D. Shindell, A. Stohl, and S. G. Warren, "Short-lived pollutants in the Arctic: Their climate impact and possible mitigation strategies," Atmos. Chem. Phys. **8**, 1723–1735 (2008).
6. J. Sandradewi, A. S. Prevot, S. Szidat, N. Perron, M. R. Alfarra, V. A. Lanz, E. Weingartner, and U. Baltensperger, "Using aerosol light absorption measurements for the quantitative determination of wood burning and traffic emission contributions to particulate matter," Environ. Sci. Technol. **42**, 3316–3323 (2008).
7. S. K. Grange, H. Lotscher, A. Fischer, L. Emmenegger, and C. Hueglin, "Evaluation of equivalent black carbon source apportionment using observations from Switzerland between 2008 and 2018," Atmos. Meas. Tech. **13**, 1867–1885 (2020).
8. S. Yue, J. Zhu, S. Chen, Q. Xie, W. Li, L. Li, H. Ren, S. Su, P. Li, and H. Ma, "Brown carbon from biomass burning imposes strong circum-Arctic warming," One Earth **5**, 293–304 (2022).
9. C. Zhu, Y. Kanaya, M. Takigawa, K. Ikeda, H. Tanimoto, F. Taketani, T. Miyakawa, H. Kobayashi, and I. Pisso, "FLEXPART V.10.1 simulation of source contributions to Arctic black carbon," Atmos. Chem. Phys. **20**, 1641–1656 (2020).
10. P. Zenkova, D. Chernov, V. Shmargunov, M. Panchenko, and B. Belan, "Submicron aerosol and absorbing substance in the troposphere of the Russian sector of the Arctic according to measurements onboard the TU-134 Optik aircraft laboratory in 2020," Atmos. Ocean. Opt. **35**, 43–51 (2022).
11. J. Schmale, S. Sharma, S. Decesari, J. Pernov, A. Massling, H.-C. Hansson, K. Von Salzen, H. Skov, E. Andrews, and P. K. Quinn, "Pan-Arctic seasonal cycles and long-term trends of aerosol properties from 10 observatories," Atmos. Chem. Phys. **22**, 3067–3096 (2022).
12. J.-D. Paris, A. Stohl, P. Nedelec, M. Y. Arshinov, M. Panchenko, V. Shmargunov, K. S. Law, B. Belan, and P. Ciais, "Wildfire smoke in the Siberian Arctic in summer: Source characterization and plume evolution from airborne measurements," Atmos. Chem. Phys. **9**, 9315–9327 (2009).
13. M. Manousakas, O. Popovicheva, N. Evangeliou, E. Diapouli, N. Sitnikov, N. Shonija, and K. Eleftheriadis, "Aerosol carbonaceous, elemental and ionic composition variability and origin at the Siberian high Arctic, Cape Baranova," Tellus B: Chem. Phys. Meteorol. **72**, 1–14 (2020).
14. S. M. Sakerin, L. P. Golobokova, D. M. Kabanov, D. A. Kalashnikova, V. S. Kozlov, I. A. Kruglinskii, V. I. Makarov, A. P. Makshtas, S. A. Popova, V. F. Radionov, G. V. Simonova, Yu. S. Turchinovich, T. V. Khodzher, O. I. Khuriganova, O. V. Chankina, and D. G. Chernov, "Measurements of physicochemical characteristics of atmospheric aerosol at research Station Ice Base Cape Baranov in 2018," Atmos. Ocean. Opt. **32** (5), 511–520 (2018) 2019.
15. V. Romanenkov, D. Rukhovich, P. Koroleva, and J. L. McCarty, "Estimating black carbon emissions from agricultural burning," in *Novel Measurement and Assessment Tools for Monitoring and Management of Land and Water Resources in Agricultural Landscapes of Central Asia* (Springer, 2014), pp. 347–364.
16. M.-H. Cho, R. J. Park, J. Yoon, Y. Choi, J. I. Jeong, L. Labzovskii, J. S. Fu, K. Huang, S.-J. Jeong, and B.-M. Kim, "A missing component of Arctic warming: Black carbon from gas flaring," Environ. Res. Lett. **14**, 094011 (2019).
17. A. Stohl, Z. Klimont, S. Eckhardt, K. Kupiainen, V. P. Shevchenko, V. M. Kopeikin, and A. N. Novigatsky, "Black carbon in the Arctic: The underestimated role of gas flaring and residential combustion emissions," Atmos. Chem. Phys. **13**, 8833–8855 (2013).
18. A. Stohl, E. Andrews, J. Burkhart, C. Forster, A. Herber, S. Hoch, D. Kowal, C. Lunder, T. Mefford, and J. Ogren, "Pan-Arctic enhancements of light absorbing aerosol concentrations due to North American boreal forest fires during summer 2004," J. Geophys. Res.: Atmos. **111**, D11306 (2006).
19. A. Vinogradova, "Anthropogenic black carbon emissions to the atmosphere: Surface distribution through Russian territory," Atmos. Ocean. Opt. **28** (2), 158–164 (2015).
20. O. B. Popovicheva, N. Evangeliou, K. Eleftheriadis, A. C. Kalogridis, N. Sitnikov, S. Eckhardt, and A. Stohl, "Black carbon sources constrained by observations in the Russian high Arctic," Environ. Sci. Technol. **51**, 3871–3879 (2017).
21. J. Schacht, B. Heinold, J. Quaas, J. Backman, R. Cherian, A. Ehrlich, A. Herber, W. T. K. Huang, Y. Kondo, A. Massling, P. R. Sinha, B. Weinzierl, M. Zanatta, and I. Tegen, "The importance of the representation of air pollution emissions for the modeled distribution and

radiative effects of black carbon in the Arctic," Atmos. Chem. Phys. **19**, 11159–11183 (2019).

22. O. Popovicheva, E. Diapouli, A. Makshtas, N. Shonija, M. Manousakas, D. Saraga, T. Uttal, and K. Eleftheriadis, "East Siberian Arctic background and black carbon polluted aerosols at HMO Tiksi," Sci. Total Environ. **655**, 924–938 (2019).
23. P. Winiger, A. Andersson, S. Eckhardt, A. Stohl, I. P. Semiletov, O. V. Dudarev, A. Charkin, N. Shakhova, Z. Klimont, C. Heyes, and O. Gustafsson, "Siberian Arctic black carbon sources constrained by model and observation," Proc. Nat. Acad. Sci. U.S.A. **114**, E1054–E1061 (2017).
24. P. Winiger, A. Andersson, S. Eckhardt, A. Stohl, and O. Gustafsson, "The sources of atmospheric black carbon at a European gateway to the Arctic," Nat. Commun. **7**, 1–8 (2016).
25. O. B. Popovicheva, V. O. Kobelev, A. I. Sinitskii, N. M. Sitnikov, M. A. Chichaeva, and A. Khansen, "Urban emissions of black carbon in the Arctic region by observations near Salekhard city," Opt. Atmos. Okeana **33** (9), 690–697 (2020).
26. O. B. Popovicheva, N. Evangeliou, V. O. Kobelev, M. A. Chichaeva, K. Eleftheriadis, A. Gregoric, and N. S. Kasimov, "Siberian Arctic black carbon: Gas flaring and wildfire impact," Atmos. Chem. Phys. **22**, 5983–6000 (2022).
27. L. Drinovec, G. Mocnik, P. Zotter, A. Prevot, C. Ruckstuhl, E. Coz, M. Rupakheti, J. Sciare, T. Muller, and A. Wiedensohler, "The "dual-spot" aethalometer: An improved measurement of aerosol black carbon with real-time loading compensation," Atmos. Meas. Tec. **5**, 1965–1979 (2015).
28. Y. Zhang, J. Schnelle-Kreis, G. Abbaszade, R. Zimmermann, P. Zotter, R. R. Shen, K. Schaefer, L. Shao, A. S. Prevot, and S. Szidat, "Source apportionment of elemental carbon in Bejing, China. Insights from radiocarbon and organic marker measurements," Environ. Sci. Technol. **49**, 8408–8415 (2015).
29. G. A. Allen, P. J. Miller, L. J. Rector, M. Brauer, and J. G. Su, "Characterization of valley winter woodsmoke concentrations in northern NY using highly time-resolved measurements," Aerosol Air Qual. Res. **11**, 519–530 (2011).
30. Y. Wang, P. K. Hopke, O. V. Rattigan, X. Xia, D. C. Chalupa, and M. J. Utell, "Characterization of residential wood combustion particles using the two-wavelength aethalometer," Environ. Sci. Technol. **45**, 7387–7393 (2011).
31. K. Eleftheriadis, S. Nyeki, C. Psomiadou, and I. Colbeck, "Background aerosol properties in the European Arctic," Water, Air Soil Pollut.: Focus **4**, 23–30 (2004).
32. A. Stein, R. Draxler, G. Rolph, B. Stunder, M. Cohen, and F. Ngan, "NOAA'S HYSPLIT atmospheric transport and dispersion modeling system," Bull. Am. Meteorol. Soc. **96**, 2059–2077 (2015).
33. R. R. Draxler and G. Hess, "An overview of the HYSPLIT_4 modelling system for trajectories," Aust. Meteorol. Mag. **47**, 295–308 (1998).
34. K. A. Shukurov, O. V. Postylyakov, A. N. Borovski, L. M. Shukurova, A. N. Gruzdev, A. S. Elokhov, V. V. Savinykh, I. I. Mokhov, V. A. Semenov, and O. G. Chkhetiani, "Study of transport of atmospheric admixtures and temperature anomalies using trajectory methods at the A.M. Obukhov Institute of Atmospheric Physics," Proc. IOP Conf. Series: Earth Environ. Sci. **231**, 012048 (2019). https://doi.org/10.1088/1755-1315/231/1/012048
35. R. S. Stone, S. Sharma, A. Herber, K. Eleftheriadis, and D. W. Nelson, "A characterization of Arctic aerosols on the basis of aerosol optical depth and black carbon measurements," Elem. Sci. Anth. **2**, 000027 (2014).
36. S. Sharma, D. Lavoue, H. Cachier, L. Barrie, and S. Gong, "Long-term trends of the black carbon concentrations in the Canadian Arctic," J. Geophys. Res.: Atmos. **109**, D15203 (2004).
37. S. Eckhardt, B. Quennehen, D. J. L. Olivie, T. K. Berntsen, R. Cherian, J. H. Christensen, W. Collins, S. Crepinsek, N. Daskalakis, M. Flanner, A. Herber, C. Heyes, O. Hodnebrog, L. Huang, M. Kanakidou, Z. Klimont, J. Langner, K. S. Law, M. T. Lund, R. Mahmood, A. Massling, S. Myriokefalitakis, I. E. Nielsen, J. K. Nojgaard, J. Quaas, P. K. Quinn, J.-C. Raut, S. T. Rumbold, M. Schulz, S. Sharma, R. B. Skeie, H. Skov, T. Uttal, K. von Salzen, and A. Stohl, "Current model capabilities for simulating black carbon and sulfate concentrations in the Arctic atmosphere: A multimodel evaluation using a comprehensive measurement data set," Atmos. Chem. Phys. **15**, 9413–9433 (2015).
38. K. Huang, J. S. Fu, E. L. Hodson, X. Dong, J. Cresko, V. Y. Prikhodko, J. M. Storey, and M.-D. Cheng, "Identification of missing anthropogenic emission sources in Russia: Implication for modeling Arctic haze," Aerosol Air Qual. Res. **14**, 1799–181 (2014).
39. A. A. Vinogradova, N. S. Smirnov, and V. N. Korotkov, "Anomalous wildfires in 2010 and 2012 on the territory of Russia and supply of black carbon to the Arctic," Atmos. Ocean. Opt. **29** (5), 545–550 (2016).

Translated by O. Bazhenov